

30 π Aromatic Meso-Substituted Heptaphyrin Isomers: Syntheses, Characterization, and Spectroscopic Studies

Venkataramanarao G. Anand,[†] Simi K. Pushpan,[†] S. Venkatraman,[†]
 Seenichamy Jeyaprakash Narayanan,^{†,‡} Abhishek Dey,[†] Tavarekere K. Chandrashekar,^{*,†}
 Raja Roy,[§] Bhavani S. Joshi,[§] S. Deepa,^{||} and G. Narahari Sastry^{||}

*Department of Chemistry, Indian Institute of Technology, Kanpur, India, NMR Division,
 Central Drug Research Institute, Lucknow, India, and Department of Chemistry,
 Pondicherry University, Pondicherry, India*

tkc@iitk.ac.in

Received April 2, 2002

The syntheses of new aromatic 30 π heptaphyrins either through a [5 + 2] or a [4 + 3] acid-catalyzed condensation and oxidative coupling reactions of easily available and air-stable precursors are reported. The methodology followed is not only simple and efficient but also allows synthesis of a range of heptaphyrins with different heteroatoms in the core. The oxidative coupling reactions of modified tripyrranes **11** and tetrapyrroles **12** were found to be dependent on the acid concentration used and as well as the substituents present on the meso position. The change of meso aryl substituents in **11** and **12** to meso mesityl substituents gave a new heptaphyrin **18**. The structural characterization has been done with extensive ¹H and 2D NMR studies. The heptaphyrins reported here show rich structural diversity when the connections of the heterocyclic rings are altered, and accordingly, one ring and two ring inversions have been observed. By a judicious choice of the precursors it has been possible to control the site of ring inversion either in the bithiophene unit or in the tripyrrane unit. Theoretical calculations performed on three different heptaphyrins, **4**, **5**, and **17**, also reveal that the inverted structures are ~35–40 kJ lower in energy relative to the corresponding noninverted structures. Furthermore, one of the heptaphyrins **10c** shows the presence of two conformers in solution in the ratio 1:2 and no interconversion between the conformers have been observed in the temperature range of 343–228 K. On protonation, the aromaticity and the ring inversions are retained and the $\Delta\delta$ values vary in the range 10.07–20.59 ppm. The energies of the Soret maxima and the HOMO–LUMO gap vary linearly with the increase in π electrons further justifying the aromatic nature of the heptaphyrins.

Introduction

Expanded porphyrins are a class of macrocyclic compounds in which heterocyclic units such as pyrrole/thiophene/furan/selenophene rings are linked to each other in a cyclic fashion through meso carbon bridges.¹ Unlike a porphyrin ring, which is an 18 π system, the expanded porphyrins contain more than 18 π electrons in their conjugated pathway. There are two general types of expanded porphyrins known in the literature. In the first case, the number of π electrons can be increased by increasing the number of conjugated double bonds linking the pyrrole/heterocyclic unit as in 26 π bisvinyllogous porphyrin **1** (Chart 1).^{1,2} Alternatively, the number of π

electrons can be increased by increasing the number of heterocyclic rings in the macrocycle as in 26 π rubyrin **2**.³ Expanded porphyrins belonging to first type are important from the point of view of aromaticity and cis–trans disposition of conjugated double bonds.^{1b} The second type of expanded porphyrins is important from the point of view of metal coordination⁴ due to the increased number of heteroatoms, varying cavity sizes, and the aromaticity in these macrocycles depends on the nature and number of links bridging the heterocyclic unit. Further interest in such macrocycles arises from their use as metal sequestering agents, contrast agents in MRI, RNA cleaving catalysts for antisense applications, en-

[†] Indian Institute of Technology.

[‡] Current address: Medicinal Chemistry, University Hospital, Arizona State University, Tempe, AZ.

[§] Central Drug Research Institute.

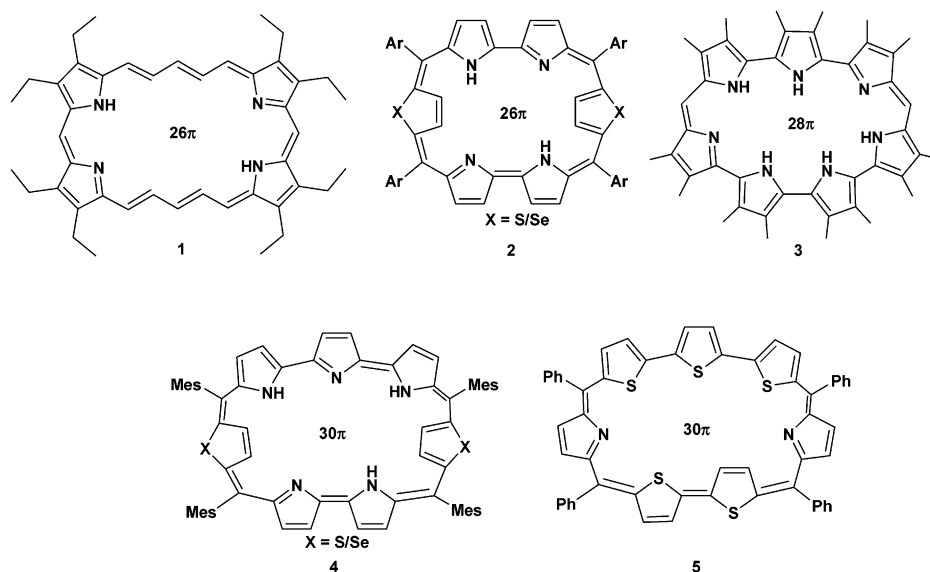
^{||} Pondicherry University.

(1) (a) For a recent highlight on expanded porphyrins, see: Sessler, J. L.; Weghorn, S. J. *Expanded, Contracted and Isomeric Porphyrins*; Elsevier: Oxford, U.K., 1997; and references therein. (b) Sessler, J. L.; Gebauer, A.; Weghorn, S. J. *Expanded Porphyrins*. In *Porphyrin Handbook*; Kadish, K. M., Smith, K. M., Guillard, R., Eds.; Academic Press: New York, 2000. (c) Lash, T. D. *Angew. Chem., Int. Ed.* **2000**, *39*, 1763.

(2) (a) Wessel, T.; Franck, B.; Möller, M.; Rodewald, U.; Läge, M. *Angew. Chem., Int. Ed. Engl.* **1993**, *32*, 1148. (b) Knübel, G.; Franck, B. *Angew. Chem., Int. Ed. Engl.* **1988**, *27*, 1170.

(3) (a) Sessler, J. L.; Morishima, T.; Lynch, V. *Angew. Chem., Int. Ed. Engl.* **1991**, *30*, 977. (b) Srinivasan, A.; Reddy, V. M.; Narayanan, S. J.; Sridevi, B.; Pushpan, S. K.; Kumar, M. R.; Chandrashekar, T. K. *Angew. Chem., Int. Ed. Engl.* **1997**, *36*, 2598. (c) Narayanan, S. J.; Sridevi, B.; Chandrashekar, T. K.; Vij, A.; Roy, R. *J. Am. Chem. Soc.* **1999**, *121*, 9053. (d) Srinivasan, A.; Pushpan, S. K.; Kumar, M. R.; Chandrashekar, T. K.; Roy, R. *Tetrahedron* **1999**, 6671. (e) Narayanan, S. J.; Sridevi, B.; Chandrashekar, T. K.; Vij, A.; Roy, R. *Angew. Chem., Int. Ed.* **1998**, *37*, 3394.

CHART 1



zyme models, anion binding agents, and sensitizers for PDT.^{1b,5}

There are only a few reports on the expanded porphyrins containing more than six heterocyclic rings. They are 28 π heptaphyrin **3** and 32 π and 30 π octaphyrin reported by Sessler and co-workers,^{6a,b} 34 π , 36 π , and 38 π octaphyrins,⁷ 40 π 10 pyrrolic turcasarin,⁸ 48 π 12 pyrrolic dodecaphyrin, 64 π 16 pyrrolic hexadecaphyrin,^{9a} 80 π icosaphyrin, and 96 π tetracosaphyrin.^{9b} Furuta and co-workers were also successful in synthesizing expanded porphyrins in a Rothmund type condensation of pyrrole and aldehyde.¹⁰ Even though these expanded porphyrins are important from structural point of view where they exhibit various nonplanar or figure eight twisted conformations, they all turned out to be nonaromatic systems.

Very recently Sessler and co-workers^{6c} have reported the synthesis of a 30 π aromatic heptaphyrin, which exhibits a flat structure in solution and a figure eight nonplanar structure in the solid state. The aromaticity in these macrocycles depends on the number and the nature of the link between the heterocyclic rings as well as the flexibility of the ring. For example, the antiaromatic character of **3** was attributed to the presence of five direct pyrrole–pyrrole links in the structure,^{6a} while the adaptation of figure eight conformation disrupts the π electron pathway in octaphyrins.⁷

The characterization of aromatic expanded porphyrins containing 30 π or higher systems still remains a challenge not only from the synthetic point of view but also from an understanding of molecular and electronic structures of the macrocycle, which can give more insight into the π -conjugation pathway. Recently in a preliminary report,¹¹ we described the successful synthesis of aromatic 30 π heptaphyrins by a judicious choice of the precursors. More recently, we were also successful in the synthesis of an aromatic 34 π octaphyrin that exhibits a flat structure.¹² In this paper, we wish to report on the characterization of a range of aromatic 30 π heptaphyrins synthesized either through acid-catalyzed type condensation reactions¹³ or through an oxidative coupling of appropriate precursors. It has been shown that the heptaphyrins exhibit rich structural diversity where different types of ring inverted structures have been characterized through detailed ¹H and 2D NMR studies. In one case, two different structural conformers have been observed and both of them exhibit an aromatic nature. Ab initio calculations indicated lower energies for the inverted structures, and the energy-optimized structures show excellent agreements with structures derived from the solution NMR data.

(4) (a) Sessler, J. L.; Seidel, D.; Vivian, E. A.; Lynch, V.; Scott, L. B.; Keogh, D. W. *Angew. Chem., Int. Ed.* **2001**, *40*, 591. (b) Sessler, J. L.; Weghorn, S. J.; Hiseada, Y.; Lynch, V. *Chem.–Eur. J.* **1995**, *1*, 56. (c) Narayanan, S. J.; Sridevi, B.; Chandrashekar, T. K.; Englich, U.; Senge, K. R. *Inorg. Chem.* **2001**, *40*, 1637. (d) Sridevi, B.; Narayanan, S. J.; Rao, R.; Chandrashekar, T. K.; Englich, U.; Senge, K. R. *Inorg. Chem.* **2000**, *39*, 3669. (e) Sessler, J. L.; Gebauer, A.; Hoehner, M.; Lynch, V. *Chem. Commun.* **1998**, 1835. (f) Weghorn, S. J.; Sessler, J. L.; Lynch, V.; Baumann, T. F.; Sibert, J. W. *Inorg. Chem.* **1996**, *35*, 1089. (g) Sessler, J. L.; Gebauer, A.; Scherer, M.; Lynch, V.; *Inorg. Chem.* **1998**, *37*, 2703.

(5) For various applications of expanded porphyrins, see: Sessler, J. L.; Weghorn, S. J. *Expanded, Contracted and Isomeric Porphyrins*; Elsevier: Oxford, U.K., 1997; Chapter 10 and references therein.

(6) (a) Sessler, J. L.; Seidel, D.; Lynch, V. *J. Am. Chem. Soc.* **1999**, *121*, 11257. (b) Bucher, C.; Seidel, D.; Lynch, V.; Sessler, J. L. *Chem. Commun.* **2002**, 328. (c) Seidel, D.; Lynch, V.; Sessler, J. L. *Angew. Chem., Int. Ed.* **2002**, *41*, 1422.

(7) (a) Vogel, E.; Broring, M.; Fink, J.; Rosen, D.; Schmickler, H.; Lex, J.; Chan, K. W. K.; Wu, Y.-D.; Plattner, D. A.; Nendel, M.; Houk, K. N. *Angew. Chem., Int. Ed. Engl.* **1995**, *34*, 2511. (b) Broring, M.; Jendry, J.; Zander, L.; Schmickler, H.; Lex, J.; Wu, Y.-D.; Nendel, M.; Chen, J.; Plattner, D. A.; Houk, K. N.; Vogel, E. *Angew. Chem., Int. Ed. Engl.* **1995**, *34*, 2515. (c) Werner, A.; Michels, M.; Zander, L.; Lex, J.; Vogel, E. *Angew. Chem., Int. Ed.* **1999**, *38*, 3650. (d) Sprutta, N.; Latos-Grazynski, L. *Chem.–Eur. J.* **2001**, *7*, 5099. (e) Kozaki, M.; Parakka, J.; Cava, M. P. *J. Org. Chem.* **1996**, *61*, 3657.

(8) Sessler, J. L.; Weghorn, S. J.; Lynch, V.; Johnson, M. R. *Angew. Chem., Int. Ed. Engl.* **1994**, *33*, 1509.

(9) (a) Setsune, J. L.; Katakami, Y.; Iizuna, N. *J. Am. Chem. Soc.* **1999**, *121*, 8957. (b) Setsune, J. L.; Maeda, S. *J. Am. Chem. Soc.* **2000**, *122*, 12405.

(10) Shin, J.-Y.; Furuta, H.; Yoza, K.; Igarashi, S.; Osuka, A. *J. Am. Chem. Soc.* **2001**, *123*, 7190.

(11) Anand, V. G.; Pushpan, S. K.; Srinivasan, A.; Narayanan, S. J.; Sridevi, B.; Chandrashekar, T. K.; Roy, R.; Joshi, B. S. *Org. Lett.* **2000**, *2*, 3829.

(12) Anand, V. G.; Pushpan, S. K.; Venkatraman, S.; Dey, A.; Chandrashekar, T. K.; Roy, R.; Joshi, B. S.; Teng, W.; Senge, K. R. *J. Am. Chem. Soc.* **2001**, *123*, 8620.

(13) Lash, T. D. *Chem.–Eur. J.* **1996**, *2*, 1197.

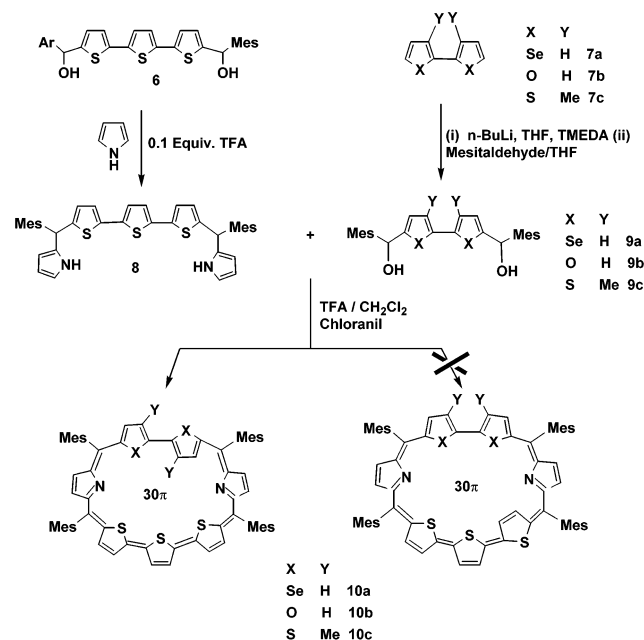
Results and Discussion

(a) Syntheses and Characterization: Condensation Reactions. From an understanding of literature it can be hypothesized that the two important parameters responsible for sustaining the diatropic ring current in expanded porphyrins are the number of heterocyclic rings and the number of meso carbons used for forming the macrocyclic ring. Altering the number of either one of them at a time has invariably led to the successful synthesis of aromatic expanded porphyrins.¹¹ The recent report of planar, aromatic 34 π octaphyrins reported from this laboratory supports such a hypothesis.¹² In sharp contrast, simultaneous variation of both the parameters disrupts the aromatic ring current either due to the flexibility of the molecule or to the increased number of direct pyrrole–pyrrole links found for octaphyrins and higher order cyclopolypyrroles.^{6–10} With this understanding, reactions were tested to synthesize 30 π aromatic macrocycles with only four meso carbon atoms and a greater number of heterocyclic rings as discussed below.

In general, expanded porphyrins are synthesized either through an acid-catalyzed condensation or oxidative coupling of appropriate precursors. Currently [2 + 3],¹⁴ [4 + 1],¹⁵ [3 + 1 + 1],¹⁶ or [3 + 3]¹⁷ condensation and self-coupling of small molecules are used widely to synthesize expanded porphyrins.³ A preliminary report from this laboratory used a [4 + 3] condensation of appropriate precursors to yield a series of aromatic 30 π heptaphyrins.¹¹ On the other hand, Sessler and co-workers used a [3 + 2 + 2] oxidative coupling methodology to synthesize antiaromatic **3**.⁶ In the present methodology we have used a [5 + 2] acid-catalyzed condensation using modified pentapyrrane **8**, synthesized from terthiophene diol **6** on reaction with pyrrole in 60% yield. The other precursor chosen was biselenophene/bifuran/3,3'-dimethyl-2,2'-bithiophene diols **9a–c**, synthesized from biselenophene/bifuran/3,3'-dimethyl-2,2'-bithiophene **7a–c** on reaction with *n*-butyllithium and mesitaldehyde (Scheme 1). This β -substituted diol was chosen specifically for two reasons: (a) to understand the steric factor; (b) to distinguish the ring inversion between the terthiophene and the bithiophene moiety in the resultant macrocycle. Thus, in a typical procedure condensation of equimolar quantities of **8** and **9c**, under N₂, in the dark with 1 equiv of trifluoroacetic acid (TFA), followed by oxidation with chloranil and chromatographic separation on basic alumina with 1:1 (v/v) methylene chloride/petroleum ether, yielded the heptaphyrin **10c** in 20% yield.

Similar [5 + 2] condensations were conducted with **8** and mesityl diols of unsubstituted biselenophene **9a** and

SCHEME 1. Synthesis of Heptaphyrins through a [5 + 2] Condensation Reaction



bifuran **9b** to get aromatic heptaphyrins **10a,b** in 18% and 15% yields, respectively. The yield of these reactions did not vary much in comparison to [4 + 3] condensation reactions reported earlier.¹¹

The proposed compositions and the solution structures of the heptaphyrins **10a–c** were arrived at by the FAB mass spectral data and detailed ¹H and 2D NMR studies on the free base as well as the protonated derivatives. For example, **10b** exhibits 2 doublets in the region –0.64 to –1.46 ppm attributed to the inner CH protons of the inverted ring while, 12 doublets for the remaining 12 CH's of the heterocyclic rings are observed in the aromatic region 10.67–8.14 ppm suggesting the unsymmetrical nature of these macrocycles. Protonation retains the ring inversion, and the additional NH protons resonate in the shielded region suggesting the retainment of the diatropic ring current. Similar observation was seen in **10a** also. Further confirmation for the proposed structure comes from ⁷⁷Se NMR of **10a**.

Two sharp singlets at 537 and 557 ppm, with respect to dimethyl selenide, observed clearly suggest two different environments for the selenium nuclei, confirming the ring inversion in the biselenophene subunit (refer to the Supporting Information). The selenium chemical shifts observed have been slightly shielded relative to octaethyltetraselenaporphyrin reported by Vogel and co-workers.¹⁸

Two different structures are possible for the heptaphyrins depending on whether the inverted ring is a part of the terthiophene fragment or the bithiophene/biselenophene/bifuran fragments (Scheme 1). This ambiguity was resolved by the NMR spectrum of **10c**, where the substitution of the methyl's on the bithiophene fragment can distinguish between the two structures. **10c** exhibits an interesting NMR spectrum as depicted in Figure 1. A careful analysis of the spectrum revealed the presence

(14) (a) Srinivasan, A.; Anand, V.G.; Narayanan, S. J.; Pushpan, S. K.; Kumar, M. R.; Chandrashekar, T. K.; Sugiura, K.-I.; Sakata, Y. *J. Org. Chem.* **1999**, *64*, 8693. (b) Sessler, J. L.; Lisowski, J.; Boudreaux, K. A.; Lynch, V.; Barry, J.; Kodadek, T. *J. Org. Chem.* **1995**, *60*, 5975.

(15) (a) Bauer, V. J.; Clive, D. L.; Dolphin, D.; Paine, J. B., III; Harris, F. L.; King, M. M.; Loder, J.; Wang, S.-W. C.; Woodward, R. B. *J. Am. Chem. Soc.* **1983**, *105*, 6429. (b) Paolesse, R.; Licocchia, S.; Spagnoli, M.; Boschi, T.; Khoury, R. G.; Smith, K. M. *J. Org. Chem.* **1997**, *62*, 5137.

(16) Shevchuk, S. V.; Davis, J. M.; Sessler, J. L. *Tetrahedron Lett.* **2001**, *42*, 2447.

(17) Sessler, J. L.; Seidel, D.; Bucher, C.; Lynch, V. *Chem. Commun.* **2000**, 1473.

(18) Vogel, E.; Fröde, C.; Breihan, A.; Schmickler, H.; Lex, J. *Angew. Chem., Int. Ed. Engl.* **1997**, *36*, 2609.

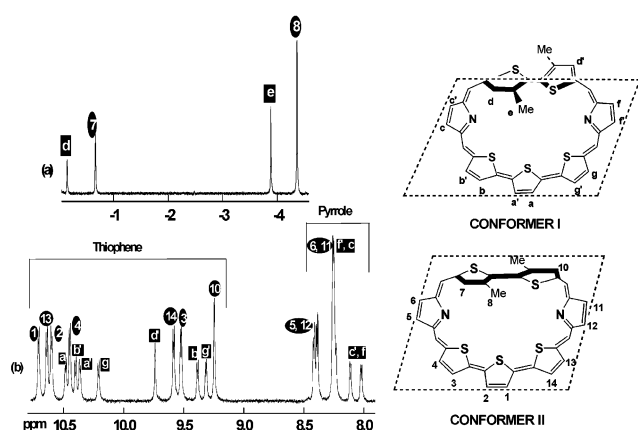


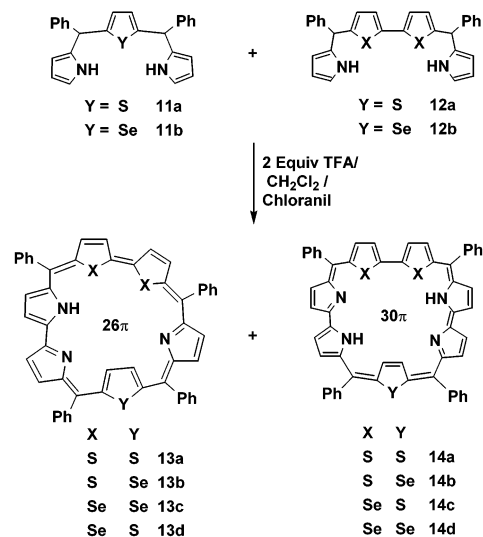
FIGURE 1. ^1H NMR of **10c** in CDCl_3 at 298K (10^{-2} M). The assignments of the (a) shielded region and (b) aromatic region are marked in numbers and letters respectively for the two conformers.

of two different conformers in the solution in the ratio 1:2. All efforts to separate the conformers were futile. The NMR assignments were based on the 2D COSY correlations (refer to Supporting Information). Specifically the number of peaks observed both in the aromatic region and the shielded region were doubled relative to **10a** or **10b**, suggesting the presence of two conformers in solution. In the upfield region, four singlets were observed between -0.1 and -4.4 ppm for the protons of the inverted thiophene ring. Of these, signals at -4.34 and -3.86 ppm are for the methyl protons, which resonate as a singlet, and the β -CH protons resonate at -0.15 and -0.64 ppm. The absence of correlation between two peaks in the ^1H - ^1H COSY confirmed their assignment and ring inversion in the bithiophene unit. Thus, the peaks at -0.64 and -4.34 ppm correspond to one of the conformers and the peaks at -0.15 and -3.86 ppm correspond to the other conformer. The methyl protons of the noninverted thiophene ring are observed at 4.02 and 2.7 ppm for the two different conformers, respectively.

In the aromatic region the pyrrole protons and the thiophene protons are well separated (Figure 1). Six sets of doublets and two singlets observed in the region 10.71–9.2 ppm are assigned to the thiophene protons. The pyrrole protons resonate as eight doublets in the region 8.4–7.9 ppm. The signal at 8.25 ppm is an overlap of pyrrole proton signals of both the conformers as revealed from 2D COSY correlations. The two singlets observed at 9.24 and 9.77 ppm correspond to hydrogen present on the noninverted ring of bithiophene unit (d' and 10).

Two different conformers of **10c** can be envisaged as follows. In conformer I, the thiophene rings of the bithiophene unit are above and below the mean macrocyclic plane, and in conformer II, both the thiophene rings of the thiophene unit are in the same plane as depicted (Figure 1). When the two rings are out of plane with each other, there will be minimum steric hindrance, while when they are in the same plane, the thiophene rings have to be planar. Thus the inverted methyl and the CH protons should experience more shielding for conformer II because of the diatropic ring current relative to conformer I, as observed in the NMR spectrum. It is pertinent to point out here that the aromatic 34π meso

SCHEME 2. Synthesis of Heptaphyrins through a [4 + 3] Coupling Reaction

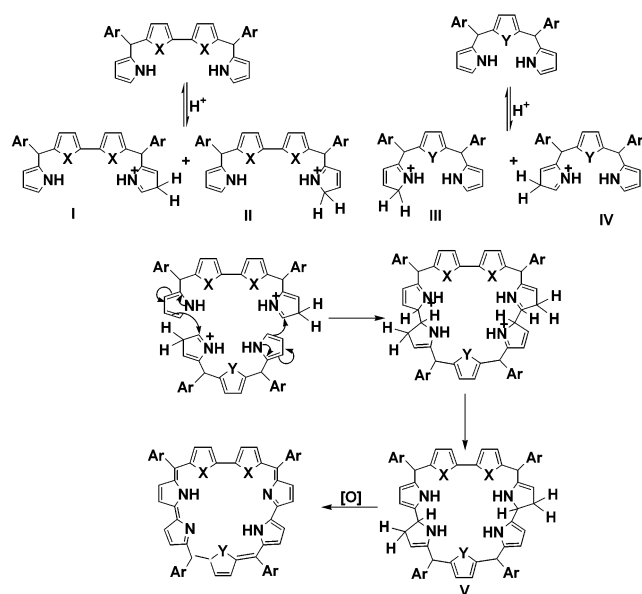


aryl octaphyrins earlier reported from this laboratory¹² show the presence of planar and nonplanar conformers in solution due to NH tautomerism.

The possibility of interconversion of one conformer to another was also studied by variable-temperature studies from 343 to 223 K for **10c**. The spectrum recorded in this range at various temperatures did not show any difference either in the chemical shifts or in the intensity of the peaks revealing that the interconversion between the two is not possible in this temperature range (refer Supporting Information). Furthermore the protonation of pyrrole nitrogens by careful titration of TFA also showed the presence of two different conformers. For the protonated derivative of conformer I the inner pyrrole NH's were observed at -5.5 and -7.06 ppm, while for the conformer II they were at -6.96 and -7.09 ppm. The β -CH protons and the inner methyl protons experienced further shielding on protonation (the β -CH and methyl group were observed at -4.67 and -7.13 ppm for conformer I and at -5.39 and -7.69 ppm for conformer II, respectively), suggesting that these protons experience more diatropic ring current upon protonation. The $\Delta\delta$ (difference between the most deshielded and shielded signals) calculated for conformer I was 19.87 ppm, while for conformer II it was 20.59 ppm revealing the aromatic nature of the macrocycle (refer to the Supporting Information).

(b) Syntheses and Characterization: Oxidative Coupling Reactions. The successful synthesis of aromatic 30π heptaphyrins encouraged us to synthesize the isomers of heptaphyrins using appropriate precursors through oxidative coupling reactions. Recently we and others have shown that oxidative coupling reactions are useful to create a direct pyrrole–pyrrole link^{6,19} in the synthesis of expanded porphyrins. In this study we have followed [4 + 3] methodology to synthesize a range of 30π heptaphyrin using appropriate precursors (Scheme 2). In a specific reaction, equimolar quantities of **11a** and **12a**, under nitrogen, were stirred with 2 equiv of TFA in

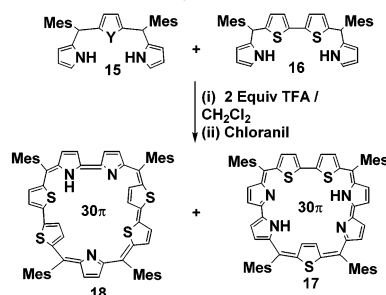
(19) Narayanan, S. J.; Sridevi, B.; Chandrashekar, T. K.; Englich, U.; Senge, K. R. *Org. Lett.* **1999**, *1*, 587.

SCHEME 3. Proposed Mechanism for the Formation of Heptaphyrins through a [4 + 3] Coupling Reaction


absence of light for 1 h, followed by chloranil oxidation and reflux for 1 h in methylene dichloride. After the usual workup and chromatographic separation on basic alumina, **14a** was isolated in 20% yield. A new isomer of rubyrin **13a** was also isolated in 3% yield. Through this methodology we were able to vary the number and orientation of heteroatoms, in more than one way, in the core of the macrocycle.

In these coupling reactions it was found that the nature and the yield of the product formed were dependent on the concentration of the acid catalyst. For example, use of 0.3 equiv of TFA resulted in formation of only rubyrin **2** in 15% yield while at 1 equiv of TFA both rubyrin **2** and **14a** were formed in 6% and 12% yield, respectively. Upon increase of the TFA concentration to 1.5 equiv, 9% of **14a**, 1% of **2**, and 11% of **13a** were formed. All these observations imply that the yield of rubyrin **2** decreases with the increase in acid concentration and tetrapyrrene reacts only at concentrations of TFA beyond 1 equiv. It is well-known that tripyrranes and tetrapyrrenes undergo acidolysis in the presence of TFA and the extent of acidolysis depends on the concentration of TFA in the reaction mixture.²⁰ Consequently the protonation of **11** and **12** leads to the intermediates **I** and **II** or **III** and **IV**, respectively. The formation of heptaphyrin now can be explained by choosing the β -protonated intermediates **I** and **IV**²⁰ to form heptaphyrinogen **V** as shown in Scheme 3, which on oxidation with chloranil gives the expected heptaphyrin.

Substitution of bulkier mesityl groups for the phenyl groups in the precursors **11** and **12** had a profound effect on the product distribution. A [3 + 4] oxidative coupling reaction of the mesityl derivatives **15** and **16** yielded a new heptaphyrin isomer **18** (Scheme 4). The reactions were carried out under similar conditions as mentioned

SCHEME 4. One-Step Synthesis of 17 and 18


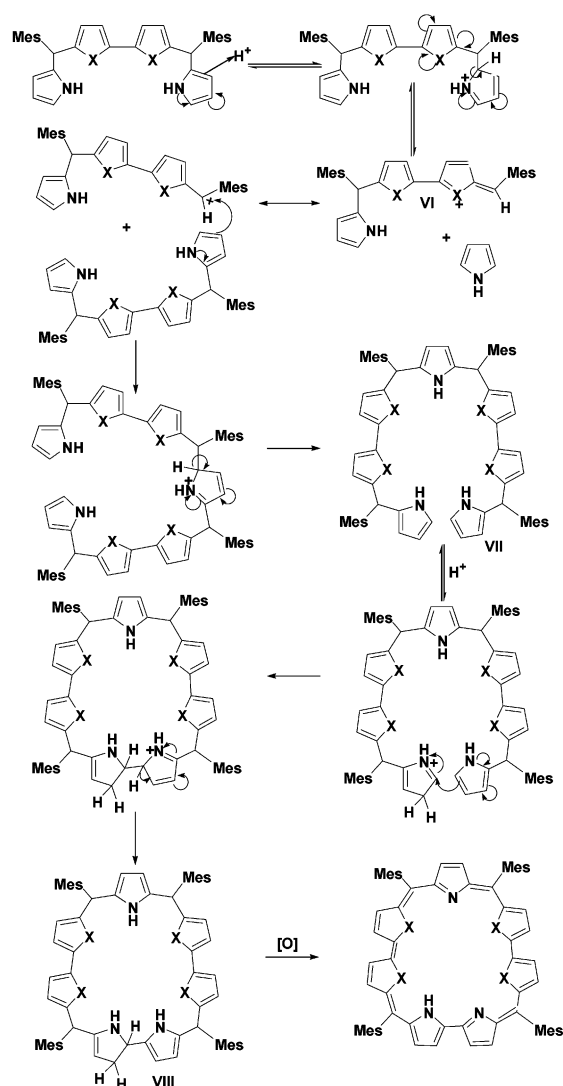
above to obtain **18** in 8–9% yield along with the expected mesityl-substituted heptaphyrin **17** in 10% yield. Heptaphyrin **18** shows a distinct feature in chromatographic separation. Generally, heptaphyrins are eluted with methylene chloride or much higher polar solvents. However, in this reaction **18** was eluted with 4:1 (v/v) methylene chloride/petroleum ether. This reaction can be seen as analogous to the formation of sapphyrin from the acidolysis of tripyrrromethanes.^{3e}

The formation of **18** can be explained only by the acidolysis of **16**, which is unknown to date. Protonation of **16** with TFA leads to fragmentation to form the reactive intermediate **VI** (Scheme 5). Through an intermolecular attack, **VI** reacts with unfragmented **16**, which on further modification forms the linear chain **VII**. On further protonation of **VII**, the β -CH of one of the pyrrole rings gets protonated and further intramolecular rearrangement leads to the formation of cyclic intermediate **VIII**. The isolation of this intermediate was not successful, as it gets oxidized to aromatic form.²⁰ Heptaphyrin **18** was obtained on oxidizing the cyclic intermediate **VIII** with chloranil. Interestingly **16** alone with up to 1.5 equiv of TFA yielded 34 π octaphyrin in higher yields and only a trace amount of **18** could be isolated. On increase of the TFA concentration to more than 2 equiv, only core-modified rubyrin^{3d} was isolated.

The important observation is only mesityl-substituted precursors yielded the heptaphyrins **4** and **18**. This clearly indicates that the presence of bulkier substituents on the meso position is necessary for the formation of bigger aromatic molecules. A similar approach was also used in the synthesis of higher cyclooctapolyrroles, i.e., octaphyrins, dodecaphyrins, and hexadecaphyrins.⁹ It is assumed that the bulkier groups on the meso positions helps the macrocyclic ring to expand more rather than to form smaller rings due to the possible steric hindrance between the β -CH protons of the heterocyclic ring and the meso substituents. In general we observed that different 30 π heptaphyrins could be achieved by tuning either the acid catalyst concentration or the meso substituents. The unexpected formation of novel macrocycles such as **13** and **18** is a clear indication that minor modifications in precursors and experimental conditions are important tools in synthesizing higher analogues of aromatic expanded porphyrins. Being the first report of acidolysis of **16**, it is now being exploited to synthesize higher analogues of expanded porphyrins.

The solution structure of **18** was arrived at by a detailed analysis of its ¹H and 2D NMR spectra both in the free base and in the protonated forms. The spectra obtained for the protonated form of **18** in the upfield

(20) (a) Lash, T. D.; Chaney, S. T.; Richter, D. T. *J. Org. Chem.* **1998**, *63*, 9076. (b) Lee, C. H.; Lindsey, J. S. *Tetrahedron* **1994**, *50*, 11427. (c) Lindsey, J. S.; Wagner, R. W. *J. Org. Chem.* **1989**, *54*, 828.

SCHEME 5. Mechanism for the Formation of Heptaphyrins through Acidolysis of Tetrapyrane


region and the aromatic region are shown in Figure 2 along with assignments made. There is a rapid tautomerism going on in the free base form, and we are unable to detect the NH signal even at 233 K.

This observation suggests that the NH proton is located on one of the bipyrrrole nitrogens (rings A and B) and not on the pyrrole ring of the tripyrrole unit (ring E) (Figure 2). This observation is also consistent with our earlier work on core-modified sapphyrins^{3e} and rubyrins. However on protonation this tautomerism is not possible and the signals due to NH protons are observed in the shielded region. Furthermore in the shielded region there are four doublets in the region 0 to -1.3 ppm in the free base of **18** and in the protonated form these doublets are further shielded and appear at -3.34 to -3.38 ppm. This observation suggests that the two of the heterocyclic rings are inverted, which is typical of meso aryl expanded porphyrins.^{3,21} In the aromatic region there are 10 clear doublets suggesting the inequivalence of all the noninverted ring protons.

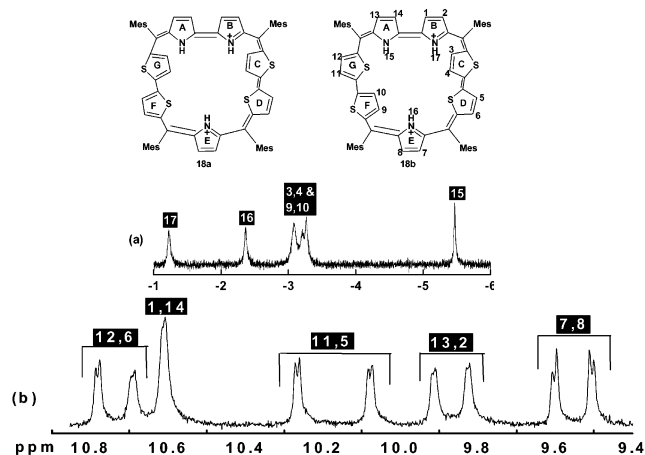


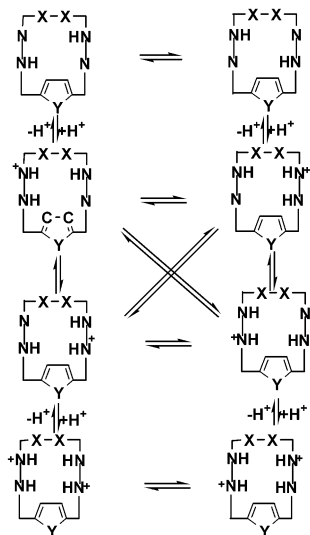
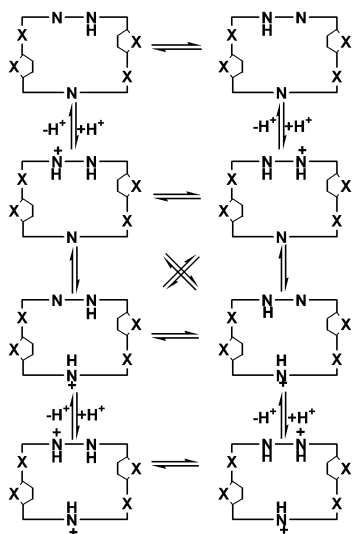
FIGURE 2. ^1H NMR of a 10^{-2} M with TFA (**18**- 2H^+) in CDCl_3 at 233 K. Protonation was done by careful addition of TFA in CDCl_3 . The assignments based on ^1H - ^1H COSY correlations are marked for the (a) shielded region and (b) aromatic region.

From our earlier experience on the inverted expanded porphyrins, we envisage two different inverted structures for **18**. One possibility is that one ring in each bithiophene unit (C and G) is inverted making the molecule more symmetric as shown in **18a** (Figure 2). The second possibility is where two different rings (C and F) are inverted making the molecule unsymmetrical as in **18b**. The observation of 10 doublets in the aromatic region suggests more unsymmetrical nature, and we conclude that the structure shown in **18b** is more appropriate in the present case. This is also supported by the observation of three different NH signals in the shielded region for the pyrrole NH protons (Figure 2). Such ring inversions in bithiophene has been observed in the case of 34 π octaphyrins.¹²

NH Tautomerism in Heptaphyrins. The possibility of the existence of different tautomeric forms of heptaphyrins was examined by recording the NMR of the free base and the protonated derivatives. Heptaphyrins **10** are not expected to show any NH tautomerism since there are no inner NH protons in the free base form. On the other hand, heptaphyrins **14**, **17**, and **18** show NH tautomerism in the free base form. The fact that the inner pyrrole NH protons were not observed in the shielded region even at 233 K suggests the existence of rapid tautomerism in **14**. There are two NH protons, one each located on the two different bipyrrrole units. It is expected that these protons exchange sites between the nitrogens of the same bipyrrrole unit. On diprotonation two different types of NH protons are observed in the shielded region due to the arresting of tautomerism. The protonation scheme observed for heptaphyrins **14/17** are depicted in Scheme 6.

The heptaphyrin **18** contains only one pyrrole hydrogen, and theoretically this could be present either on the pyrrole nitrogen of the tripyrrole unit or on one of the pyrrole nitrogens of the bipyrrrole unit. If it is located on the pyrrole nitrogen of the tripyrrole unit, NH tautomerism is not possible and one would expect to observe this signal in the shielded region. On the other hand, if it is located on one of the nitrogens of the bipyrrrole unit, NH tautomerism is possible where the proton can exchange sites between the two bipyrrrole nitrogens. If the rate of

(21) Chmielewski, P. J.; Latos-Grazynski, L.; Rachlewicz, K. *Chem.-Eur. J.* **1995**, *1*, 68.

SCHEME 6. Proposed Protonation Scheme for 14/17 by TFA**SCHEME 7. Protonation of 18 by TFA**

exchange is faster on the NMR time scale, this signal is generally not seen until the tautomerism is arrested. The fact that no signals were observed for the NH in the shielded region, even at 233 K, suggests that the NH proton is located on the nitrogens of the bipyrolo unit. As expected, upon diprotonation three different NH signals were seen, at -1.44 , -2.6 , and -5.6 ppm, at room temperature due to the arresting of tautomerism, and the protonation scheme is depicted in Scheme 7.

UV–Vis Spectral Studies. UV–vis spectral studies on heptaphyrins reveal the presence of intense Soret type of bands in the region 540–580 nm and Q type bands in the region 650–1050 nm. The presence of a greater number of heteroatoms and the effect of extended delocalization relative to 26π rubeprins and 22π sapphyrins are reflected in the red shift of the absorption bands. The ϵ values for the Soret bands were of the order of 10^5 , those for the Q bands were of the order of 10^4 , and these values are 1 order of magnitude higher relative to the antiaromatic heptaphyrin reported by Sessler and co-workers.⁶ Furthermore, upon diprotonation (Figure 3) the absorp-

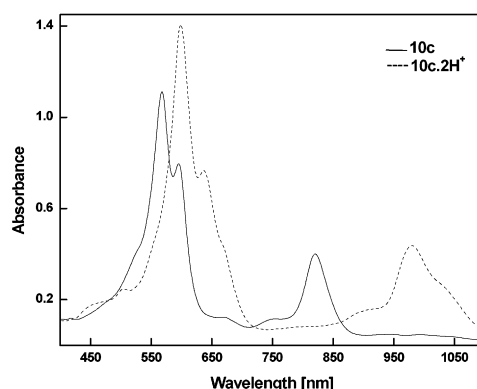


FIGURE 3. Electronic absorption spectra of **10c** (2.4×10^{-6} M) and its dication in methylene chloride. The dication was generated by careful addition of TFA.

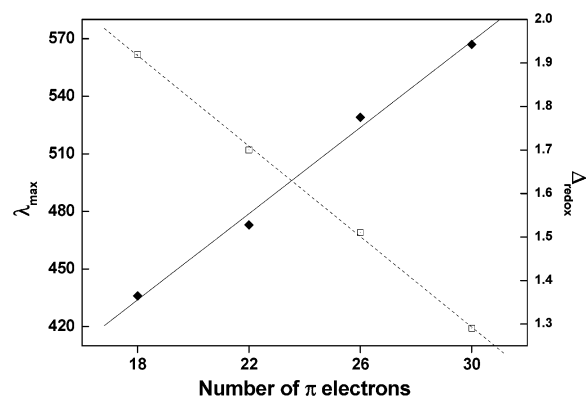


FIGURE 4. Variation of energy of the Soret band (\blacklozenge) and HOMO–LUMO gap (\square) with increasing number of π electrons.

tion bands experiences further red shift (by 30 to 45 nm), which is typical of meso aryl expanded porphyrins, and the ϵ values for the protonated derivatives are slightly higher relative to the freebase.²²

The aromaticity of these heptaphyrins can be gauged by two parameters: (a) the energy of the Soret maximum, which is expected to go down as the number of π electrons are increased in the delocalization pathway; (b) the HOMO–LUMO²³ gap, which is also expected to reduce linearly with increase in π electrons in the delocalization pathway. Such a variation for both the parameters is shown in Figure 4, where a linear correlation has been observed for both the parameters supporting the aromatic nature of the heptaphyrins reported in this work. Further support for the aromatic nature also comes from the observed $\Delta\delta$ values, which vary in the range 10.07 to 20.59 ppm for the heptaphyrins.²⁴

(22) (a) Srinivasan, A.; Anand, V. G.; Pushpan, S. K.; Chandrashekar, T. K.; Sugiura, K.-I.; Sakata, Y. *J. Chem. Soc., Perkin Trans. 2* **2000**, 1788. (b) Rachlewicz, K.; Sprutta, N.; Latos-Grazynski, L.; Chmielewski, P. J.; Szterenber, L. *J. Chem. Soc., Perkin Trans. 2* **1998**, 959.

(23) Cyclic voltametric studies of heptaphyrins in methylene chloride show two quasi-reversible reductions and two irreversible oxidations. The Δ_{redox} values have been calculated from the difference between the first oxidation and reduction potentials. See the following: (a) Srinivasan, A. Ph.D Thesis, IIT Kanpur. (b) Pushpan, S. K. Ph.D. Thesis, IIT Kanpur.

(24) Generally the aromaticity of expanded porphyrins can be measured by the difference in the chemical shifts of the inner and the outer protons, and these values vary in the range 10 to 26 ppm for various expanded porphyrins. For details, see ref 2.

TABLE 1. Summary of Theoretical Calculations

heptaphyrin	no. of inverted rings	B3LYP/ 6-31G	AM1(NIMG) ^a	IOMO
4	0	0.0	0.0 (0)	0.0
	TS (0-1)		1.1 (1)	
	1	-16.3	-15.4 (1)	-35.1
	TS (1-2)		9.7 (1)	
5	2	-36.5	-31.8 (0)	-80.4
	0	0.0	0.0 (0)	0.0
17a	1	-36.3	-14.6 (0)	-64.1
	0	0.0	0.0 (1)	0.0
	1	-40.9	-29.2 (0)	-60.9

^a The number of imaginary frequencies is indicated in parentheses.

(c) Theoretical Calculations. Failure to obtain good single crystals for X-ray structure determination forced us to use the energy optimization techniques to arrive at the possible structures for the heptaphyrins reported here. Computations were performed to understand the origin for inversion in the observed structures for **4**, **5**, and **17**. Full geometry optimizations, without imposing any symmetry constraints, are carried out at 3LYP/6-31G level of theory, which was found to provide good descriptions of porphyrin chemistry.²⁵

However, the semiempirical AM1 method is employed to obtain the barrier heights and to estimate the effect of *meso*-phenyl substitutions. All the DFT calculations were done using Gaussian 94 suite of programs,²⁶ and the semiempirical calculations were done using the MOPAC 2000 program package.²⁷ The results are compiled in Table 1. First, the heptaphyrin **4**, where both the thiophene rings are inverted, is undertaken. Figure 5 depicts the relative stabilities of the inverted and noninverted structures along with barriers.

Thus, the calculations indicate that the zero- and singly-inverted structures also correspond to minima on the potential energy surface although the double-inverted structures are more stable. Importantly, the inversion barrier is found to be low, thus indicating rapid interconversion to the most stable doubly-inverted structure. Clearly, the heptaphyrin skeleton in **4** has an inherent preference to have the doubly-inverted structure over the singly-inverted and noninverted structures. However, it is interesting to estimate how the *meso* aryl substitutions affect the relative energies of the various minimum energy structures depicted in Figure 5.

Accordingly, the effects of phenyls on the relative stability of the inverted and noninverted isomers were estimated by using Morokuma's IMOMO approach,²⁸ where the total energy is given as $E(\text{IMOMO}) =$

(25) Ghosh, A.; Wondimagegn, T.; Nilsen, H. J. *J. Phys. Chem. B* **1998**, *102*, 10459. (b) Szterenberg, L.; Latos-Grazynski, L. *J. Phys. Chem. A* **1999**, *103*, 3302.

(26) Frisch, M. J.; Trucks, G. W.; Schlegel, H. B.; Gill, P. M. W.; Johnson, B. G.; Robb, M. A.; Cheeseman, J. R.; Keith, T.; Petersson, G. A.; Montgomery, J. A.; Ragavachari, K.; Al-Laham, M. A.; Zakrzewski, V. G.; Ortiz, J. V.; Foresman, J. B.; Cioslowski, J.; Stefanov, B. B.; Nanayakkara, A.; Challacombe, M.; Peng, C. Y.; Ayala, P. Y.; Chen, W.; Wong, M. W.; Andres, J. L.; Replogle, E. S.; Gomperts, R.; Martin, R. L.; Fox, D. J.; Binkley, J. S.; Defrees, D. J.; Baker, J.; Stewart, J. P.; Head-Gordon, M.; Gonzalez, C.; Pople, J. A. *Gaussian 94*; Gaussian, Inc.: Pittsburgh, PA, 1995.

(27) Stewart, J. J. P. *MOPAC 2000*; Fujitsu Limited: Tokyo, 1999.

(28) (a) Humbel, S.; Sieber, S.; Morokuma, K. *J. Chem. Phys.* **1996**, *105*, 1959. (b) Svensson, M.; Humbel, S.; Sieber, S.; Morokuma, K. *J. Chem. Phys.* **1996**, *105*, 3654.

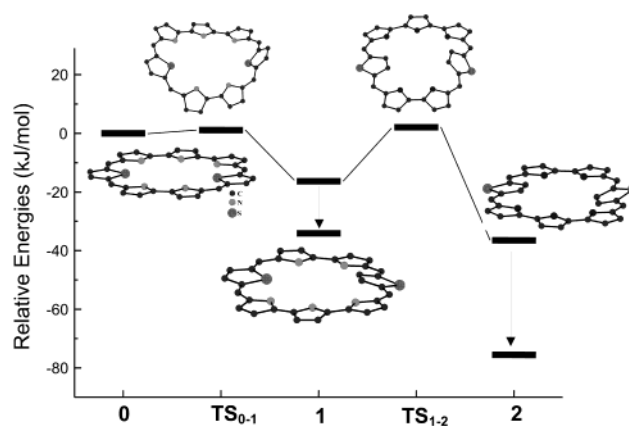


FIGURE 5. Inversion energy profile for **4**. Numbers in the axis correspond to the number of inverted rings. Solid lines connect the energies of model compound where the *meso* aryls are substituted by hydrogens. The dotted arrows indicate the energy stabilization due to the *meso* aryl substitution.

$E(\text{B3LYP, model}) + [E(\text{AM1, real}) - E(\text{AM1, model})]$, where the real and model correspond to with and without *meso* aryl substitutions, respectively. This approach will single out the contributions of the *meso* aryl substitutions on the relative stabilities of inverted isomers with respect to the noninverted structures. The energy differences between the planar and minimum energy structures are within 4 kJ mol⁻¹ in all the cases considered in the study at the B3LYP/6-31G level, although semiempirical calculations show larger deviations from planarity.

Similarly, calculations on the system **4** skeleton (replacing Hs for *meso* aryl substituents) indicate that the noninverted structure is 36 kJ mol⁻¹ higher in energy compared to the singly-inverted structure, which is also in good agreement with the experimental assignment. The singly-inverted structure **17** is also computed to be about 41 kJ mol⁻¹ compared to the noninverted structure.²⁹ Thus, the heptaphyrin skeletons studied here have a strong preference for the inverted structures over the noninverted structures.

The IMOMO calculations indicate that the *meso* phenyl substitution further increases the thermodynamic stability of the inverted structure on the order of 28 and 20 kJ mol⁻¹ over the noninverted structures in systems **5** and **17**, respectively. It is gratifying to note that the optimized structures in Figure 6 are in excellent agreement with the proposed structures on the basis of the solution NMR spectral data.

Conclusions

We were successful in synthesizing a variety of aromatic 30 π heptaphyrins and characterized with a variety of spectroscopic techniques. Our understanding to maintain four *meso* carbons as the basic skeleton for the synthesis of aromatic expanded porphyrins, while increasing the number of heterocyclic rings, has paid off.

(29) While local minima exist on the potential energy surfaces for both inverted and noninverted structures for **4** and **5**, all our attempts to obtain a C₁ stationary point were futile and lead to the singly-inverted structure. Therefore, the energy differences are taken by enforcing planarity on the zero-inverted structure. It indicates that the barrier for inversion in system **18** is zero or negligible.

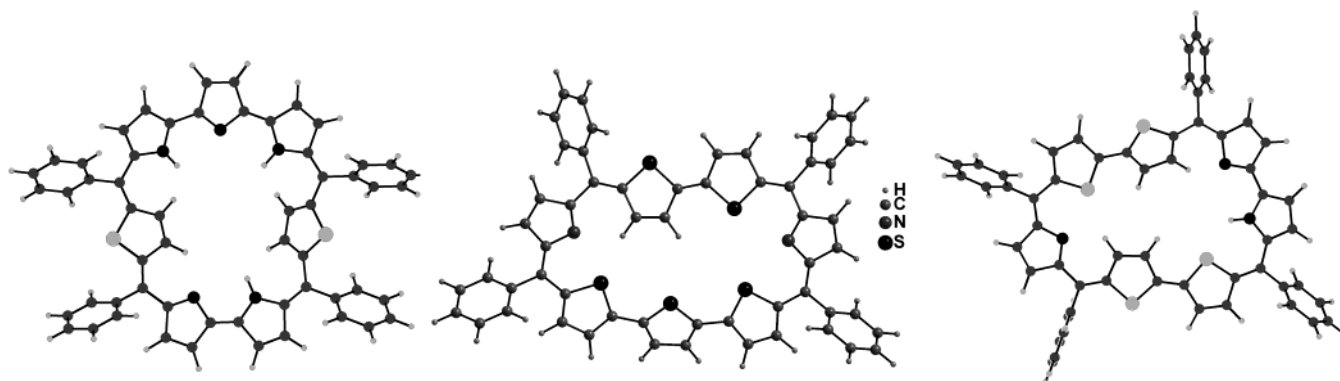


FIGURE 6. Geometry-optimized structures for **4**, **5**, and **18**. All the calculations were done with meso phenyl substituents.

These syntheses show that minor variations in the precursors and reaction conditions are crucial for obtaining novel aromatic macrocycles. Also for the first time the acidolysis of tetrapyrane has been observed for the formation of a novel 30 π macrocycle. The β -substituted thiophene was used effectively to elucidate the exact structure of the heptaphyrins, thereby giving a proper understanding into the structural diversities of these exotic macrocycles. The above-mentioned work has been a pioneering approach to understand the rich structural diversities of 30 π aromatic macrocycles. The results of theoretical studies have further supported the analysis and the structural elucidation that have been carried out. These results have given a strong impetus to carry out reactions to obtain huge aromatic molecules, for which their synthesis has been a really daunting task, and of course to study the novel and exotic properties of such systems.

Experimental Section

All the chemicals used for the syntheses were reagent grade unless otherwise specified. Solvents for spectroscopic measurements were purified and dried according to standard methods.

Syntheses. **7c**¹⁹ was synthesized by a Ni(dppp)Cl₂-catalyzed Grignard coupling reaction of 3-methyl-2-bromothiophene. **6**,¹¹ **7a**,^{3b} **7b**,^{3b} **11**,¹³ **12**,^{3b} **15**,^{3c} and **16**¹¹ were synthesized according to known procedures.

5,5'-Bis(mesitylhydroxymethyl)-2,2'-biselenophene (9a). To a solution of *N,N,N,N*-tetramethylethylenediamine (3 mL, 11.4 mmol) in dry *n*-hexane (50 mL) was added *n*-butyllithium (7.5 mL, 11.4 mmol) followed by **7a** (1 g, 3.8 mmol) under an argon atmosphere. The reaction mixture was stirred at room temperature for 1 h and later heated under reflux for 1 h. The reaction mixture was then allowed to attain 25 °C. Mesitylaldehyde (1.4 mL, 9.5 mmol) in dry tetrahydrofuran (20 mL) was added over a period of 30 min to the reaction mixture at 0 °C. After addition was over the reaction mixture was allowed to attain 25 °C and saturated aqueous ammonium chloride (25 mL) was added. It was then extracted with ether (50 mL). The organic layers were combined and washed with brine (25 mL) and dried over anhydrous Na₂SO₄. The crude product on evaporation of the solvent was recrystallized from dry toluene to afford the diol as a yellow solid. Yield: 1.45 g, 70%. Anal. Calcd for C₂₈H₃₀O₂Se₂: C, 60.44; H, 5.43. Found: C, 60.46; H, 5.39. ¹H NMR (400 MHz, CDCl₃): δ 6.9 (d, *J* = 3.96 Hz, 2H), 6.78 (s, 4H), 6.5 (m, 2H), 6.39 (s, 2H), 2.27 (s, 12H), 2.2 (s, 6H), 1.51 (br s, 2H). EI MS: *m/z* 556 (38%) [M⁺].

3,3'-Dimethyl-5,5'-bis(mesitylhydroxymethyl)-2,2'-bithiophene (9c). The above-mentioned procedure was followed with 1.9 mmol of **7c**, 5.7 mmol of *N,N,N,N*-tetrameth-

ylethylenediamine, 5.7 mmol of *n*-butyllithium, and 4.7 mmol of mesitaldehyde to obtain the diol. Yield: 0.5 g, 50%. ¹H NMR (400 MHz, CDCl₃): δ 6.82 (s, 2H), 6.78 (s, 4H), 6.35 (s, 2H), 2.5 (s, 6H), 2.27 (s, 12H), 2.25 (s, 6H), 1.54 (s, 2H). EI MS: *m/z* 490 (61%) [M⁺]. Anal. Calcd for C₃₀H₃₄O₂S₂: C, 73.43; H, 6.98. Found: C, 73.41; H, 7.01.

5,5'-Bis(mesitylhydroxymethyl)-2,2'-bifuran (9b). An earlier described procedure was followed with 7.45 mmol of **7b**, 22.3 mmol of *N,N,N,N*-tetramethylethylenediamine, 22.3 mmol of *n*-butyllithium, and 18.6 mmol of mesitaldehyde to get 1.75 g (50% yield) of the diol. ¹H NMR (400 MHz, CDCl₃): δ 6.77 (s, 4H), 6.5 (d, *J* = 3.4 Hz, 2H), 6.18 (d, *J* = 3.4 Hz, 2H), 5.9 (s, 2H), 2.27 (s, 12H), 2.2 (s, 6H), 1.56 (br s, 2H). EI MS: *m/z* 430 [M⁺] (100%). Anal. Calcd for C₂₈H₃₀O₄: C, 78.11; H, 7.02. Found: C, 78.14; H, 7.06.

Terthiapentapyrrene 8. A mixture of 0.5 g (0.92 mmol) of **6** and 36 mmol of pyrrole was degassed by bubbling with nitrogen for 10 min, and then 0.092 mmol of TFA was added. The reaction mixture was stirred for 30 min at room temperature. It was diluted with 50 mL of CH₂Cl₂ followed by a wash with 0.1 N NaOH and a water wash. The organic layer was dried over anhydrous Na₂SO₄, the solvent was removed under reduced pressure, and the unreacted pyrrole was removed by vacuum distillation at room temperature. The resulting viscous dark brown liquid was purified by column chromatography (silica gel 100–200 mesh, 6:94 EtOAc/petroleum ether). A brownish yellow band eluted and gave a light brown colored solid identified as **8**. Yield: 0.35 g. ¹H NMR (400 MHz, CDCl₃): δ 7.8 (br s, 2NH), 6.9 (d, 3.9 Hz, 2H), 6.86 (s, 2H), 6.8 (s, 4H), 6.67 (m, 2H), 6.6 (m, 2H), 6.1 (m, 2H), 6.04 (m, 2H), 5.96 (s, 2H), 2.21 (s, 6H), 2.07 (s, 12H). ES MS: *m/z* 642 [M⁺] (100%). Anal. Calcd for C₄₀H₃₈N₂S₃: C, 74.73; H, 5.96; N, 4.36. Found: C, 74.70; H, 5.93; N, 4.4.

General Procedure for Condensation Reactions: 5-, 10,19,24-Tetramesityl-33,34,35-trithia-37,38-diselenahaptaphyrin (10a). **8** (0.2 g, 0.31 mmol) and **9a** (0.17 g, 0.31 mmol) in dry CH₂Cl₂ (200 mL) were stirred under nitrogen atmosphere for 15 min at room temperature. TFA (0.025 mL, 0.31 mmol) was added to the above mixture. The solution was stirred for a further 1 h under dark conditions. The resulting solution was opened to air, chloranil (0.076 g, 0.31 mmol) was added, and the mixture was heated to reflux in a preheated oil bath for 1 h. After removal of the solvent, the crude product was purified by column chromatography (basic alumina). A deep purple band eluted with 3:1 CH₂Cl₂/petroleum ether gave a brownish metallic solid identified as **10a**. Yield: 0.065 g, 18%. **10a** decomposes above 275 °C. ¹H NMR (300 MHz, CDCl₃, 298K): δ 10.2 (d, *J* = 3 Hz, 1H), 10.08 (m, 2H), 9.84 (d, *J* = 3 Hz, 1H), 9.6 (d, *J* = 6 Hz, 1H), 9.07 (d, *J* = 6 Hz, 2H), 9.0 (d, *J* = 3 Hz, 1H), 8.07 (d, *J* = 3 Hz, 1H), 8.03 (d, *J* = 6 Hz, 1H), 7.82 (d, *J* = 6 Hz, 1H), 7.77 (d, *J* = 6 Hz, 1H), 7.3 (s, 2H), 7.23 (s, 6H), 2.57 (s, 3H), 2.56 (s, 3H), 2.55 (s, 3H), 2.54 (s, 3H), 2.2 (s, 12H), 2.04 (s, 12H), 0.0 (br s, 1H), -1.66 (br s, 1H). ¹H NMR (300 MHz, CDCl₃/TFA, 248 K): δ 12.68 (d, *J* = 6 Hz, 1H), 12.55

(d, $J = 3$ Hz, 1H), 12.41 (d, $J = 3$ Hz, 1H), 12.14 (d, $J = 6$ Hz, 1H), 11.67 (d, $J = 6$ Hz, 1H), 11.22 (d, $J = 6$ Hz, 1H), 11.08 (d, $J = 6$ Hz, 1H), 11.05 (d, $J = 6$ Hz, 1H), 9.83 (d, $J = 6$ Hz, 1H), 9.78 (s, 2H), 9.64 (d, $J = 6$ Hz, 1H), 7.68 (s, 2H), 7.61 (s, 2H), 7.6 (s, 2H), 7.59 (s, 2H), 2.82 (s, 3H), 2.8 (s, 3H), 2.78 (s, 3H), 2.77 (s, 3H), 2.19 (s, 6H), 1.95 (s, 6H), 1.93 (s, 6H), 1.9 (s, 6H), -0.75 (d, $J = 6$ Hz, 1H), -4.92 (d, $J = 6$ Hz, 1H), -6.27 (br s, NH), -6.34 (br s, NH). ^{77}Se NMR (CDCl_3 , 298 K): δ 557 (s) and 537 (s). UV-vis (CH_2Cl_2) [λ_{max} (nm) ($10^4\epsilon$): 571 (16.7), 677 (1.7), 731 (1.8), 797 (4.6); ($\text{CH}_2\text{Cl}_2/\text{TFA}$) 610 (30.4), 637 (14.8), 853 (0.9), 901 (1.5), 965 (6.1). FAB MS: m/z 1158. Anal. Calcd for $\text{C}_{68}\text{H}_{58}\text{N}_2\text{S}_3\text{Se}_2$: C, 70.57; H, 5.05; N, 2.42. Found: C, 70.54; H, 5.02; N, 2.43.

5,10,19,24-Tetramesityl-33,34,35-trithia-37,38-dioxahaptaphyrin (10b). **8** (0.1 g, 0.15 mmol) and **9b** (0.08 g, 0.15 mmol) in CH_2Cl_2 (100 mL) were subjected to conditions similar to those mentioned above with TFA (0.01 mL, 0.15 mmol) and chloranil (0.04 g, 0.15 mmol). Purification by column chromatography on basic alumina gave a purple colored band with 95:5 $\text{CH}_2\text{Cl}_2/\text{EtOAc}$ identified as **10b**, which yielded a brownish metallic solid on evaporation of solvent. Yield: 0.025 g, 15%. **10b** decomposes above 280 °C. ^1H NMR (300 MHz, CDCl_3 , 298K): δ 10.67 (d, $J = 6$ Hz, 1H), 10.46 (d, $J = 6$ Hz, 1H), 10.17 (d, $J = 6$ Hz, 1H), 9.85 (d, $J = 3$ Hz, 1H), 9.49 (d, $J = 3$ Hz, 1H), 9.37 (d, $J = 3$ Hz, 1H), 8.78 (d, $J = 6$ Hz, 1H), 8.31 (s, 2H), 8.26 (d, $J = 3$ Hz, 1H), 8.14 (d, $J = 3$ Hz, 1H), 7.45 (s, 2H), 7.3 (s, 3H), 7.26 (s, 3H), 2.67 (s, 6H), 2.63 (s, 6H), 2.6 (s, 12H), 2.58 (s, 12H), -0.64 (d, $J = 3$ Hz, 1H), -1.41 (d, $J = 3$ Hz, 1H). ^1H NMR (300 MHz, CDCl_3/TFA , 258 K): δ 12.33 (d, $J = 3$ Hz, 1H), 12.07 (d, $J = 3$ Hz, 1H), 11.56 (d, $J = 6$ Hz, 1H), 11.37 (d, $J = 3$ Hz, 1H), 10.96 (d, $J = 3$ Hz, 1H), 10.75 (d, $J = 6$ Hz, 1H), 10.15 (d, $J = 6$ Hz, 1H), 9.79 (d, $J = 6$ Hz, 1H), 9.58 (s, 2H), 9.43 (d, $J = 3$ Hz, 1H), 7.7 (s, 2H), 7.57 (s, 2H), 7.56 (s, 2H), 7.51 (s, 2H), 2.85 (s, 3H), 2.79 (s, 3H), 2.75 (s, 3H), 2.73 (s, 3H), 2.26 (s, 6H), 1.99 (s, 6H), 1.86 (s, 6H), 1.85 (s, 6H), -4.68 (s, 1H), -4.71 (s, 1H), -4.87 (br s, NH), -5.77 (br s, NH). UV-vis (CH_2Cl_2) [λ_{max} (nm) ($10^4\epsilon$): 555 (76.4), 581 (51.2), 637 (0.96), 660 (0.82), 805 (25.5); ($\text{CH}_2\text{Cl}_2/\text{TFA}$) 586 (78.5), 635 (36.5), 656 (0.96), 909 (1.4), 946 (24.1), 1015 (1.4). FAB MS: m/z 1032 [M^+] (100%). Anal. Calcd for $\text{C}_{68}\text{H}_{58}\text{N}_2\text{S}_3\text{O}_2$: C, 79.19; H, 5.67; N, 2.72. Found: C, 79.23; H, 5.62; N, 2.69.

5,10,19,24-Tetramesityl-13,16-dimethyl-33,34,35,37,38-pentathiaheptaphyrin (10c). **8** (0.2 g, 0.31 mmol) and **9c** (0.15 g, 0.31 mmol) were subjected to conditions similar to those mentioned above with TFA (0.025 mL, 0.31 mmol) and chloranil (0.075 g, 0.31 mmol). Purification by column chromatography on basic alumina gave a purple colored band with 3:2 $\text{CH}_2\text{Cl}_2/\text{petroleum}$ ether identified as **10c**, which yielded a brownish metallic solid on evaporation of solvent. Yield: 0.07 g, 20%. **10c** decomposes above 250 °C. Data for conformer **I**: ^1H NMR (400 MHz, CDCl_3 , 298 K) δ 10.47 (d, $J = 4$ Hz, 1H), 10.4 (d, $J = 4$ Hz, 1H), 10.37 (d, $J = 4$ Hz, 1H), 10.22 (d, $J = 4$ Hz, 1H), 9.7 (s, 1H), 9.38 (d, $J = 4$ Hz, 1H), 9.24 (d, $J = 4$ Hz, 1H), 8.25 (m, 2H), 8.11 (d, $J = 4$ Hz, 1H), 8.02 (d, $J = 4$ Hz, 1H), 7.34–7.3 (m, 8H), 2.7 (s, 3H), 2.64–2.61 (m, 12H), 2.15 (m, 24H), -0.15 (s, 1H), -3.86 (s, 3H); ^1H NMR (300 MHz, CDCl_3/TFA , 228 K) δ 12.7 (d, $J = 6$ Hz, 1H), 12.54 (d, $J = 6$ Hz, 1H), 12.43 (d, $J = 3$ Hz, 1H), 12.16 (d, $J = 6$ Hz, 1H), 1.26 (d, $J = 6$ Hz, 1H), 11.05 (d, $J = 3$ Hz, 1H), 9.93 (m, 1H), 9.87 (d, $J = 3$ Hz, 1H), 9.68 (d, $J = 6$ Hz, 1H), 9.58 (d, $J = 3$ Hz, 1H), 7.68 (s, 4H), 7.56 (s, 4H), 3.14 (s, 3H), 2.8–2.75 (m, 12H), 2.14–2.0 (m, 24H), -4.67 (s, 1H), -5.51 (s, NH), -7.06 (s, NH), -7.13 (s, 3H). Data for conformer **II**: ^1H NMR (400 MHz, CDCl_3 , 298 K) δ 10.7 (d, $J = 8$ Hz, 1H), 10.65 (d, $J = 8$ Hz, 1H), 10.61 (d, $J = 8$ Hz, 1H), 10.46 (d, $J = 4$ Hz, 1H), 9.58 (d, $J = 8$ Hz, 1H), 9.53 (d, $J = 4$ Hz, 1H), 9.24 (s, 1H), 8.4 (m, 2H), 8.25 (m, 2H), 7.34–7.3 (m, 8H), 4.02 (s, 3H), 2.64 (s, 6H), 2.61 (s, 6H), 2.04 (s, 12H), 2.0 (s, 12H), -0.64 (s, 1H), -4.34 (s, 3H); ^1H NMR (300 MHz, CDCl_3/TFA , 228 K) δ 12.89 (d, $J = 3$ Hz, 1H), 12.78 (d, $J = 6$ Hz, 1H), 12.64 (d, $J = 3$ Hz, 1H), 12.37 (d, $J = 3$ Hz, 1H), 11.4 (d, $J = 6$ Hz, 1H), 11.27 (d, $J =$

3 Hz, 1H), 10.75 (s, 1H), 10.04 (d, $J = 3$ Hz, 1H), 9.99 (s, 2H), 9.93 (m, 1H), 7.63 (s, 4H), 7.6 (s, 4H), 4.82 (s, 3H), 2.85–2.8 (m, 12H), 2.14 (s, 12H), 1.93 (s, 12H), -5.39 (s, 1H), -6.96 (s, NH), -7.01 (s, NH), -7.69 (s, 3H). UV-vis (CH_2Cl_2) [λ_{max} (nm) ($10^4\epsilon$): 567 (46.6), 595 (33.6), 820 (16.8), 669 (5), 993 (1.9); ($\text{CH}_2\text{Cl}_2/\text{TFA}$) 598 (58.8), 636 (32.3), 980 (18.5). FAB MS: m/z 1092 [M^+] (100%). Anal. Calcd for $\text{C}_{70}\text{H}_{62}\text{N}_2\text{S}_5$: C, 77.02; H, 5.72; N, 2.57. Found: C, 76.99; H, 5.76; N, 2.55.

General Procedure for Coupling Reactions. Procedure and experimental details for **13a**³⁰ and **14a–d**¹¹ have already been reported elsewhere.

5,10,15,24-Tetraphenyl-29,34-dithia-31-selenahexaphyrin (13b). A mixture of tetrapyrane **12a** (0.32 g; 0.68 mmol) and 5,10-diphenyl-16-selenatripyrrane (**11b**) (0.3 g; 0.68 mmol) in dry dichloromethane (200 mL) was stirred under nitrogen atmosphere for 15 min at room temperature. Trifluoroacetic acid (0.15 g, 1.36 mmol) was added to the above mixture. The solution immediately turned dark green, and stirring was continued for another 1 h. The resulting solution was exposed to air, chloranil (0.17 g; 0.68 mmol) was added, and the mixture was heated to reflux in a preheated oil bath at 45 °C for 1 h. After removal of the solvent the crude product was purified by column chromatography using basic alumina grade III. The first fraction was a pink band which moved in 1:1 dichloromethane/petroleum ether and gave a dark green solid, which was identified as **12b** (0.12 g, 20%). The second purple band eluted with 49:1 dichloromethane/ethyl acetate gave a green solid, which was identified as **13b** (0.02 g; 4%). These compounds were recrystallized from a 1:1 dichloromethane/*n*-hexane mixture. ^1H NMR (400 MHz, CDCl_3/TFA , 298 K): δ 11.43 (d, 1H, $J = 4.4$ Hz), 11.21 (d, 1H, $J = 4.8$ Hz), 10.65 (d, 1H, $J = 4.4$ Hz), 10.53 (d, 1H, $J = 4.8$ Hz), 10.36–10.34 (m, 2H), 9.81 (d, 1H, $J = 4.4$ Hz), 9.55 (d, 1H, $J = 4.5$ Hz), 9.52 (d, 1H, $J = 4.4$ Hz), 9.34 (d, 1H, $J = 5.2$ Hz), 8.91–8.87 (m, 8H), 8.75–8.7 (m, 12H), -0.64 (s, 1H), -1.59 (s, 1H), -3.01 (d, 1H, $J = 5.1$ Hz), -3.21 (d, 1H, $J = 3.9$ Hz), -4.58 (s, 1H). UV-vis (CH_2Cl_2) [λ_{max} (nm) ($10^4\epsilon$): 530 (10.72), 652 (1.09), 708 (0.86), 807 (0.41), 909 (0.35); ($\text{CH}_2\text{Cl}_2/\text{TFA}$) 564 (16.69), 748 (0.82), 838 (1.64), 911 (1.77). FAB mass [m/z (%): 844 (50) [$\text{M} + 2$]⁺. Anal. Calcd for $\text{C}_{52}\text{H}_{33}\text{N}_3\text{S}_2\text{Se}$: C, 74.10; H, 3.95; N, 4.99. Found: C, 74.12; H, 3.93; N, 4.95.

5,10,15,24-Tetraphenyl-29,34-diselena-31-thiahexaphyrin (13c). Tetrapyrane **12b** (0.59 g; 1.04 mmol) and 5,10-diphenyl-16-thiatripyrrane (**11a**) (0.41 g; 1.04 mmol), trifluoroacetic acid (0.24 g, 2.1 mmol), and chloranil (0.51 g; 2.1 mmol) in dry dichloromethane under reaction conditions similar to those mentioned above gave **14c** (0.18 g; 19%) and **13c** (0.03 g; 3%). ^1H NMR (400 MHz, CDCl_3 , 298K): δ 11.13 (s, 2H), 10.37 (d, 1H, $J = 4.8$ Hz), 10.33 (d, 1H, $J = 4.8$ Hz), 9.67 (d, 1H, $J = 5.2$ Hz), 9.58 (d, 1H, $J = 4$ Hz), 9.03 (d, 1H, $J = 4$ Hz), 8.93 (d, 1H, $J = 4$ Hz), 8.76 (d, 1H, $J = 4.3$ Hz), 8.6 (d, 1H, $J = 4.3$ Hz), 8.47 (d, 2H, $J = 7.3$ Hz), 8.38–8.32 (m, 6H), 7.88–7.7 (m, 12H), -1.83 (s, 1H), -2.72 (s, 1H). ^1H NMR (400 MHz, CDCl_3 , TFA, 298 K): δ 11.5 (d, 1H, 4.8 Hz), 11.2 (d, 1H, $J = 5.2$ Hz), 10.95 (d, 1H, $J = 4.8$ Hz), 10.81 (d, 1H, $J = 5.2$ Hz), 10.44 (d, 1H, $J = 4.4$ Hz), 10.4 (d, 1H, $J = 4.8$ Hz), 9.82 (d, 1H, $J = 4.4$ Hz), 9.72 (d, 1H, $J = 4.4$ Hz), 9.58 (d, 1H, $J = 4.8$ Hz), 9.51 (d, 1H, $J = 5.2$ Hz), 8.97–8.93 (m, 4H), 8.85 (d, 2H, $J = 7.6$ Hz), 8.75 (d, 2H, $J = 6.4$ Hz), 8.24–7.97 (m, 12H), -1.27 (s, 1H), -2.11 (br.s, 1H), -3.49 (d, 1H, $J = 5.2$ Hz), -3.57 (d, 1H, $J = 4$ Hz), -5.49 (s, 1H). UV-vis (CH_2Cl_2) [λ_{max} (nm) ($10^4\epsilon$): 549 (8.96), 680 (0.51), 743 (0.3), 861 (0.04), 987 (0.23); ($\text{CH}_2\text{Cl}_2/\text{TFA}$) 579 (10.5), 659 (0.02), 721 (0.19), 774 (0.23), 868 (0.81), 937 (0.74). FAB mass: [m/z (%): 890 (45) [$\text{M} + 1$]⁺. Anal. Calcd for $\text{C}_{52}\text{H}_{33}\text{N}_3\text{S}_2\text{Se}_2$: C, 70.19; H, 3.14; N, 4.72. Found: C, 70.21; H, 3.09; N, 4.75.

5,10,15,24-Tetraphenyl-29,31,34-triselenahexaphyrin (13d). Tetrapyrane **12b** (0.47 g; 0.99 mmol) and 5,10-

(30) Pushpan, S. K.; Anand, V. G.; Venkatraman, S.; Srinivasan, A.; Gupta, A. K.; Chandrashekar, T. K. *Tetrahedron Lett.* **2001**, *42*, 3391.

diphenyl-16-selenatripyrrane (**11b**) (0.44 g; 0.99 mmol), trifluoroacetic acid (0.23 g, 2 mmol), and chloranil (0.49 g; 2 mmol) in dry dichloromethane under reaction conditions similar to those explained for the previous compounds gave **14d** (0.18 g; 18%) and **13d** (0.04 g; 4%). ¹H NMR (400 MHz, CDCl₃, 298 K): 11.9–11.86 (m, 2H), 11.16–11.12 (m, 2H), 10.44 (d, 1H, *J* = 4 Hz), 10.4 (d, 1H, *J* = 4.8 Hz), 9.89 (d, 1H, *J* = 4.8 Hz), 9.62 (d, 2H, *J* = 4 Hz), 9.38–9.33 (m, 7H), 9.25 (d, 2H, *J* = 6.8 Hz), 8.91–8.7 (m, 12H), 0.01 (d, 1H, *J* = 6 Hz), –1.02 (d, 1H, *J* = 6 Hz), –1.26 (br s, 1H). ¹H NMR (400 MHz, CDCl₃/TFA, 298 K): δ 11.43 (d, 1H, *J* = 4.8 Hz), 11.14 (d, 1H, *J* = 4.8 Hz), 10.94 (d, 1H, *J* = 4.8 Hz), 10.76 (d, 1H, *J* = 4.8 Hz), 10.35 (s, 1H), 10.32 (s, 1H), 9.82 (d, 1H, *J* = 4.4 Hz), 9.56 (s, 1H), 9.52 (d, 1H, *J* = 4.8 Hz), 9.34 (d, 1H, *J* = 4 Hz), 8.98 (d, 1H, *J* = 7.2 Hz), 8.87 (d, 1H, *J* = 7.2 Hz), 8.79 (d, 4H, *J* = 6.4 Hz), 8.26–8.03 (m, 12H), –0.73 (s, 1H), –1.61 (br.s, 1H), –3.3 (s, 1H), –3.12 (s, 1H), –4.54 (br s, 1H). UV–vis (CH₂Cl₂) [λ_{\max} (nm) (10⁴ ϵ): 548 (14.55), 675 (0.91), 734 (0.38), 850 (0.11), 973 (0.3); (CH₂Cl₂/TFA) 582 (16.33), 672 (0.15), 727 (0.31), 771 (0.43), 862 (1.07), 937 (1.21)]. FAB mass [*m/z* (%): 938 (25) [M + 2]⁺. Anal. Calcd for C₅₂H₃₃N₃Se₃: C, 66.68; H, 3.55; N, 4.49. Found: C, 66.64; H, 3.53; N, 4.52.

5,14,19,28-Tetramesityl-34,35,37,38-tetrathiaheptaphyrin (18). Tetrapyrane **16** (0.4 g, 0.71 mmol) and tripyrrane **15** (0.34 g, 0.71 mmol) in dry CH₂Cl₂ (200 mL), in the dark, were stirred under nitrogen atmosphere for 15 min at room temperature. TFA (0.11 mL, 1.4 mmol) was added to the above mixture, and the stirring was continued for another 1 h. The resulting solution was exposed to air, chloranil (0.35 g, 1.4 mmol) was added, and the mixture was heated to reflux in a preheated oil bath for 1 h. After removal of solvent, the crude

product was purified by column chromatography using basic alumina grade III. The first blue band moving in 4:1 CH₂Cl₂/petroleum ether gave a dark red solid identified as **18** (0.03 g, 5%). The second purple band eluting with 49.5:0.5 CH₂Cl₂/EtOAc gave a green solid which was identified as **17** (0.11 g, 15%). **18** decomposes above 250 °C. ¹H NMR (400 MHz, CDCl₃, 298 K): 9.95 (br s, 1H), 9.74 (br s, 1H), 9.36 (br s, 1H), 9.34 (br s, 1H), 9.3 (br s, 1H), 9.25 (br s, 1H), 8.67 (br s, 1H), 8.624 (br s, 1H), 8.34 (br s, 1H), 8.25 (br s, 1H), 0.5–7.3 (m, 8H), 2.69 (s, 6H), 2.63 (s, 6H), 2.31 (s, 12H), 2.23 (s, 12H), 0.0 (br s, 1H), –0.842 (br s, 1H), –1.11 (br s, 1H), –1.31 (br s, 1H). ¹H NMR (400 MHz, CDCl₃/TFA, 233 K): δ 10.89 (br s, 1H), 10.8 (br s, 1H), 10.7 (s, 2H), 10.4 (br s, 1H), 10.2 (br s, 1H), 10.0 (br s, 1H), 9.89 (br s, 1H), 9.67 (br s, 1H), 9.58 (br s, 1H), 7.7 (s, 4H), 7.61 (s, 2H), 7.57 (s, 2H), 2.84 (s, 6H), 2.8 (s, 6H), 2.4 (s, 12H), 2.27 (s, 12H), –1.44 (s, NH), –2.6 (s, NH), –3.34 (s, 2H), –3.38 (s, 2H), –5.6 (s, NH). UV–vis (CH₂Cl₂) [λ_{\max} (nm) (10⁴ ϵ): 581 (10.32), 813 (br), 854 (1.24); (CH₂Cl₂/TFA) 613 (12.1), 802 (0.3), 916 (0.91), 1034 (2.5)]. FAB mass [*m/z* (%): 1047 (100%) [M + 1]. Anal. Calcd for C₆₈H₅₈N₃S₄: C, 78.12; H, 5.59; N, 4.02. Found: C, 78.09; H, 5.55; N, 4.08.

Acknowledgment. The authors thank the DST, New Delhi, India, for the financial support. S.K.P. and B.S.J. thank the CSIR for a senior research fellowship.

Supporting Information Available: Selected ¹H NMR and ¹H–¹H 2D Cosy and FAB mass spectra. This material is available free of charge via the Internet at <http://pubs.acs.org>.

JO025788D